

# Unsteady Magnetohydrodynamics Natural Convection Dissipative Flow Through an Inclined Plate

\*Dada, M.S. and Aladesusi, O.S.

Department of Mathematics, University of Ilorin, Ilorin, Nigeria

Received: June 26, 2015; Revised: August 25, 2015; Accepted: September 7, 2015

## Abstract

This study investigates the effects of viscous dissipation on an unsteady two-dimensional magnetohydrodynamic (MHD) natural convection through an inclined plate. The governing partial differential equations together with the boundary conditions are transformed into a system of dimensionless coupled partial differential equations. An implicit finite difference method is used to solve the dimensionless equations. The effects of various fluid parameters on velocity, temperature, concentration distribution are separately presented in graphical forms and discussed.

**Keywords:** Viscous dissipation, MHD, Natural convection, Inclined plate, Finite difference

## 1.0 Introduction

Dissipation of energy is significant when considering the unsteady MHD natural convective flow through an inclined plate. Viscous dissipation effect is reflected by the Eckert number which is a source of the temperature rise that takes place in the flow of the fluid. Magneto hydrodynamics has an important application in several engineering problems such as MHD power generators in the boundary layer control aerodynamics, nuclear reactors cooling and also in the petroleum industries.

In view of its application, Mukhopadhyay *et al.* [1] studied MHD boundary layer flow over a heated stretching sheet with variable viscosity. Gnanaswara [2] carried out Lie group analysis of heat and mass transfer effects on steady MHD free convection dissipative fluid flow past an inclined porous surface with heat generation. Gnanaswara and Bhasker [3] investigated mass and heat generation effects on MHD free convection flow past inclined vertical surface in a porous medium while Islam *et al.* [4] carried out analysis on the MHD free convection and mass transfer flow past through an inclined plate with heat generation. The governing two-dimensional energy and mass transfer equations were obtained by boundary layer approximation. It was shown that the effects of Magnetic and Heat source parameters enhanced the velocity field. Kalpadides and Balassas [5] studied the free convective boundary layer problem of an electrically conducting fluid over an elastic surface by group theoretic method. It was found from the numerical solution that the effect of increasing thermal Grashof number is manifested by an increase in flow velocity. In the presence of a magnetic field parameter with the permeability of porous medium, viscous dissipation is demonstrated to exert a more significant effect on the flow field and thus, on the heat transfer from the plate to the fluid. The velocity and concentration is found to decrease gradually as the Schmidt number is increased.

The study of flow through a porous medium and dissipation effect has received attention of many researchers because of its extensive application in enhancing recovery of petroleum, chemical engineering etc. Sandeep and Sugunamma [6] analysed the effect of inclined magnetic field on unsteady free convective flow of dissipative fluid past a vertical plate. Dada and Adefolaju [7] investigated dissipation, MHD and radiation effects on an unsteady convective heat and mass transfer in a Darcy-Forchheimer porous medium. It was noted that temperature and concentration slightly increase with increase in magnetic field parameter while the presence of magnetic field has a retarding effect on the velocity profile. A rise in the conduction-radiation parameter causes reduction in the velocity profile while a rise in the dissipation function induces a considerable rise in velocity. Increase in the Prandtl number, Schmidt number, thermal Grashof number, solutant Grashof number and the conduction radiation parameter causes the temperature to reduce, while a rise in the Darcy number causes a rise in temperature along and normal to the wall.

Hunegnaw and Kishan [8] carried out analysis on unsteady MHD heat and mass transfer flow over stretching sheet in porous medium with variable properties considering viscous dissipation and chemical reaction while Megahed *et al.* [9] studied a similarity analysis in magnetohydrodynamics hall effects on free convection flow and mass transfer past a semi-infinite vertical flat plate.

---

\*Corresponding Author: Tel: +234(0)8033547911, Email: dadamsa@gmail.com

© 2015 College of Natural Sciences, Al-Hikmah University, Nigeria; All rights reserved.

Other researchers investigated the similarity reductions for problems of radiative and magnetic field effects on free convection and mass-transfer flow past a semi-finite flat plate [10]. They obtained new similarity reductions and found an analytic solution for the uniform magnetic field by using Lie group method. Chen [11] further analysed the natural convection flow over a permeable inclined surface with variable wall temperature and concentration.

The result showed that velocity is decreased in the presence of a magnetic field. Increasing the angle of inclination decreases the effect of buoyancy force. Heat transfer rate is increased when the Prandtl number is increased. Reddy and Reddy [12] performed an analysis to study natural convection flow over a permeable inclined surface with variable temperature, momentum and concentration. Based on the foregoing, the present study investigates the effects of viscous dissipation on MHD free convection and mass transfer flow with heat generation through an inclined plate.

**2.0 Problem Formulation**

Considering an unsteady two-dimensional MHD natural convection and dissipating fluid past an inclined plate in a Cartesian coordinate system where the X-axis is chosen along the plate in the direction of the flow and the Y-axis is normal to it. It has been considered initially that the plate as well as the fluid is at the same temperature  $T_\infty$  and the concentration levels  $C_\infty$  everywhere in the fluid. Also, it is considered that the fluid and the plate is at rest after which the plate moves with a constant velocity  $U_0$  in its own plane and instantaneously at time  $t > 0$ , the concentration and the temperature of the plate are raised to  $C_w > C_\infty$  and  $T_w > T_\infty$  respectively, where  $C_w, T_w$  are concentration and temperature at the wall of the plate respectively and  $C_\infty, T_\infty$  are the concentration and temperature far away from the plate respectively. The physical model of the problem is presented in Fig. 1.

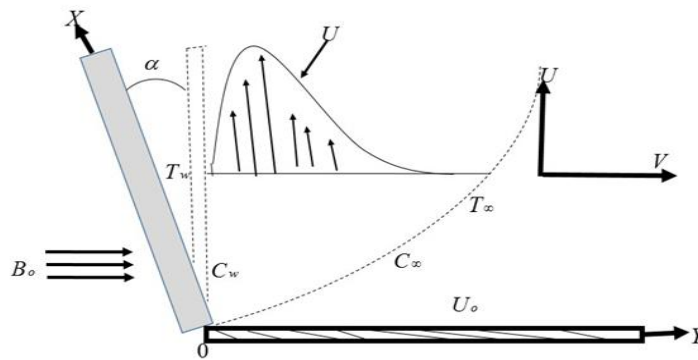


Fig. 1: The physical model and coordinate system of the flow channel

With reference to the generalized governing equations described above, the transient two-dimensional problem is governed by the following system of coupled non-linear differential equations.

$$\frac{\partial u}{\partial x} + \frac{\partial v}{\partial y} = 0 \tag{1}$$

$$\frac{\partial u}{\partial t} + u \frac{\partial u}{\partial x} + v \frac{\partial u}{\partial y} = \nu \frac{\partial^2 u}{\partial y^2} + g\beta(T - T_\infty) \cos \alpha + g\beta^*(C - C_\infty) \cos \alpha - \frac{\sigma \beta_0^2}{\rho} u \tag{2}$$

$$\frac{\partial T}{\partial t} + u \frac{\partial T}{\partial x} + v \frac{\partial T}{\partial y} = K_T \frac{\partial^2 T}{\partial y^2} + \frac{Q_r}{\rho C_p} + \frac{\mu}{\rho C_p} \left( \frac{\partial u}{\partial y} \right)^2 \tag{3}$$

$$\frac{\partial C}{\partial t} + u \frac{\partial C}{\partial x} + v \frac{\partial C}{\partial y} = D \frac{\partial^2 C}{\partial y^2} \tag{4}$$

The corresponding initial and boundary conditions are:

$$\left. \begin{aligned} \text{at } t = 0, \quad u = 0, \quad v = 0, \quad C \rightarrow C_\infty, \text{ every where} \\ u = 0, \quad v = 0, \quad T \rightarrow T_\infty, \quad C \rightarrow C_\infty \text{ at } x = 0 \end{aligned} \right\} \quad (5)$$

$$\left. \begin{aligned} \text{at } t > 0 \quad u = U_0, \quad v = 0, T \rightarrow T_\infty, \quad C \rightarrow C_\infty \text{ at } y = 0 \\ u = 0, \quad v = 0, \quad T \rightarrow T_w, \quad C \rightarrow C_w \text{ as } y \rightarrow \infty \end{aligned} \right\} \quad (6)$$

where  $x, y$  are Cartesian coordinate system,  $u$  and  $v$  are  $x$  and  $y$  components of flow velocity respectively. Here  $g$  is the local acceleration due to gravity;  $\mu$  is the dynamic viscosity;  $\rho$  is the density of the fluid;  $K$  is the thermal conductivity,  $C_p$  is the specific heat at the constant pressure;  $D$  is the coefficient of mass diffusivity;  $\beta$  and  $\beta^*$  are the thermal and concentration expansion coefficients respectively;  $\alpha$  is the angle of inclination;  $T$  is the temperature of the fluid in the boundary layer;  $\sigma$  is the electrical conductivity of the fluid;  $T_\infty$  is the temperature of the fluid far away from the plate;  $C$  is the concentration in the boundary layer;  $C_\infty$  is the concentration in the fluid far away from the surface;  $B_0$  is the magnetic induction and  $\nu$  is the kinematic viscosity.

Introducing the following dimensionless variables;

$$X = \frac{xU_0}{\nu}; Y = \frac{yU_0}{\nu}; U = \frac{u}{U_0}; V = \frac{v}{U_0}; \tau = \frac{tU_0^2}{\nu}; \bar{T} = \frac{T - T_\infty}{T_w - T_\infty}; \bar{C} = \frac{C - C_\infty}{C_w - C_\infty}; Q^* = \frac{Q_T}{(T - T_\infty)} \quad (7)$$

where  $X$  and  $Y$  are dimensionless coordinates,  $U$  and  $V$  are dimensionless velocities,  $\tau$  is the dimensionless time,  $\bar{T}$  is the dimensionless temperature function,  $\bar{C}$  is the dimensionless concentration function. By applying these dimensionless variables in equations (1) - (4), the following non dimensional equations are obtained:

$$\frac{\partial U}{\partial X} + \frac{\partial V}{\partial Y} = 0 \quad (8)$$

$$\frac{\partial U}{\partial \tau} + U \frac{\partial U}{\partial X} + V \frac{\partial U}{\partial Y} = \frac{\partial^2 U}{\partial Y^2} + G_r \bar{T} \cos \alpha + G_m \bar{C} \cos \alpha - MU \quad (9)$$

$$\frac{\partial \bar{T}}{\partial \tau} + U \frac{\partial \bar{T}}{\partial X} + V \frac{\partial \bar{T}}{\partial Y} = \frac{1}{Pr} \frac{\partial^2 \bar{T}}{\partial Y^2} + \bar{T} \cdot \gamma + E_c \left( \frac{\partial U}{\partial Y} \right)^2 \quad (10)$$

$$\frac{\partial \bar{C}}{\partial \tau} + U \frac{\partial \bar{C}}{\partial X} + V \frac{\partial \bar{C}}{\partial Y} = D \frac{\partial^2 \bar{C}}{\partial Y^2} \quad (11)$$

where

$$\frac{\nu g \beta (T_w - T_\infty)}{U_0^3} = G_r = \text{Grashof number}$$

$$\frac{\nu g \beta^* (C_w - C_\infty)}{U_0^3} = G_m = \text{Modified Grashof number}$$

$$\frac{\sigma B_0^2 \nu}{\rho U_0^2} = M = \text{Magnetic parameter}$$

$$P_r = \frac{VC_p}{k} = \text{Prandtl number}$$

$$E_c = \frac{\mu U_o^2}{C_p(T_w - T_\infty)V} = \text{Eckert number}$$

$$\gamma = \frac{VQ^*}{U_o^2 \rho C_p} = \text{Heat source parameter}$$

$$S_c = \frac{V}{D} = \text{Schmidt number}$$

Also, the associated initial and boundary conditions becomes

$$\left. \begin{array}{l} \tau = 0 \quad U = 0, \quad V = 0 \quad \bar{T} = 0 \quad \bar{C} = 0 \quad \text{everywhere} \\ U = 0, \quad V = 0 \quad \bar{T} = 0 \quad \bar{C} = 0 \quad \text{at } X = 0 \end{array} \right\} \quad (12)$$

$$\left. \begin{array}{l} \tau \rightarrow 0 \quad U = 0, \quad V = 0 \quad \bar{T} = 1 \quad \bar{C} = 1 \quad \text{at } Y = 0 \\ U = 0, \quad V = 0 \quad \bar{T} = 0 \quad \bar{C} = 0 \quad \text{as } Y \rightarrow 0 \end{array} \right\} \quad (13)$$

### 3.0 Method of Solution

We solved the unsteady non-linear coupled partial differential equations (8) to (11) subject to the conditions given in (12) and (13) by employing an implicit finite difference of the Crank-Nicolson type. The coupled non-linear partial differential equations are converted to difference equations. We defined the coordinates  $(X, Y, \tau)$  of the mesh points of the solution domain by  $X = i\Delta X$ ,  $Y = j\Delta Y$  and  $\tau = k\Delta\tau$  where  $i, j, k$  are positive integers and we denote the values of  $U$  at these mesh points by  $U(i\Delta x, j\Delta y, k\Delta\tau) = U_{i,j}^k$  and  $V(i\Delta x, j\Delta y, k\Delta\tau) = V_{i,j}^k$ . The finite difference equations corresponding to these equations are given as follows:

$$\frac{[U_{i,j}^{k+1} - U_{i-1,j}^{k+1} + U_{i,j}^k - U_{i-1,j}^k + U_{i,j-1}^{k+1} - U_{i-1,j-1}^{k+1} U_{i,j-1}^k - U_{i-1,j-1}^k]}{4\Delta X} + \quad (14)$$

$$\frac{[V_{i,j}^{k+1} - V_{i,j-1}^{k+1} + V_{i,j}^k - V_{i,j-1}^k]}{2\Delta Y} = 0$$

$$\frac{[U_{i,j}^{k+1} - U_{i,j}^k]}{\Delta\tau} + U_{i,j}^k \frac{[U_{i,j}^{k+1} - U_{i-1,j}^{k+1} + U_{i,j}^k - U_{i-1,j}^k]}{2\Delta X} +$$

$$V_{i,j}^k \frac{[U_{i,j+1}^{k+1} - U_{i,j-1}^{k+1} + U_{i,j+1}^k - U_{i,j-1}^k]}{4\Delta Y} =$$

$$\frac{[U_{i,j-1}^{k+1} - 2U_{i,j}^{k+1} + U_{i,j+1}^{k+1} + U_{i,j-1}^k - 2U_{i,j}^k + U_{i,j+1}^k]}{2(\Delta Y)^2} +$$

$$G_r \frac{[T_{i,j}^{k+1} + T_{i,j}^k]}{2} \cos \alpha + G_m \frac{[C_{i,j}^{k+1} + C_{i,j}^k]}{2} \cos \alpha - M \frac{[U_{i,j}^{k+1} + U_{i,j}^k]}{2}$$

$$\begin{aligned} & \frac{[\bar{T}_{i,j}^{k+1} - \bar{T}_{i,j}^k]}{\Delta \tau} + U_{i,j}^k \frac{[\bar{T}_{i,j}^{k+1} - \bar{T}_{i-1,j}^{k+1} + \bar{T}_{i,j}^k - \bar{T}_{i-1,j}^k]}{2\Delta X} \\ & + V_{i,j}^k \frac{[\bar{T}_{i,j+1}^{k+1} - \bar{T}_{i,j-1}^{k+1} + \bar{T}_{i,j+1}^k - \bar{T}_{i,j-1}^k]}{4\Delta Y} = \\ & \frac{1}{P_r} \frac{[\bar{T}_{i,j-1}^{k+1} - 2\bar{T}_{i,j}^{k+1} + \bar{T}_{i,j+1}^{k+1} + \bar{T}_{i,j-1}^k - 2\bar{T}_{i,j}^k + \bar{T}_{i,j+1}^k]}{2(\Delta Y)^2} \end{aligned} \tag{16}$$

$$\begin{aligned} & + \gamma \frac{[\bar{T}_{i,j}^{k+1} + \bar{T}_{i,j}^k]}{2} + E_c \left[ \frac{U_{i,j+1}^k - U_{i,j}^k}{2\Delta Y} \right]^2 \\ & \frac{[\bar{C}_{i,j}^{k+1} - \bar{C}_{i,j}^k]}{\Delta \tau} + U_{i,j}^k \frac{[\bar{C}_{i,j}^{k+1} - \bar{C}_{i-1,j}^{k+1} + \bar{C}_{i,j}^k - \bar{C}_{i-1,j}^k]}{2\Delta X} + \\ & V_{i,j}^k \frac{[\bar{C}_{i,j+1}^{k+1} - \bar{C}_{i,j-1}^{k+1} + \bar{C}_{i,j+1}^k - \bar{C}_{i,j-1}^k]}{4\Delta Y} = \\ & \frac{1}{S_c} \frac{[\bar{C}_{i,j-1}^{k+1} - 2\bar{C}_{i,j}^{k+1} + \bar{C}_{i,j+1}^{k+1} + \bar{C}_{i,j-1}^k - 2\bar{C}_{i,j}^k + \bar{C}_{i,j+1}^k]}{2(\Delta Y)^2} \end{aligned} \tag{17}$$

The region of consideration here is a rectangle with sides  $X_{(max)} (=1)$  and  $Y_{(max)}$  where  $X_{(max)}$  corresponds to  $Y = \infty$  which lies outside the momentum, thermal and concentration boundary layers. The subscripts  $i$  and  $j$  denote the grid points with  $X$  and  $Y$  coordinates respectively and  $k$  along the  $t$ -direction. Dividing  $X$  and  $Y$  into  $M$  and  $N$  grid spacing respectively, the mesh sizes are taken as  $\Delta X = 0.05$  and  $\Delta Y = 0.05$  and  $\Delta t = 0.001$ . During any one-time step, the coefficients  $U_{i,j}^k$  and  $V_{i,j}^k$  appearing in the difference equations are treated as constants. The values of  $C, T, U$  and  $V$  are known at all grid point at  $t = 0$  from the boundary/initial conditions. The values of  $C, T, U$  and  $V$  at time level  $(k + 1)$  are evaluated using the already known values at previous time level  $(k)$ .

Hence, the finite difference equations form a tridiagonal system of equations at every internal nodal point on a particular  $i$ -level which are solved by using Matlab programming package that employs Thomas Algorithm [13]. Thus, the values of  $C$  and  $T$  at every nodal point for a particular  $i$  at  $(k + 1)$  th time level were calculated and the results obtained were used in  $U$  at  $(k + 1)$  th time level. The values of  $V$  are also determined at every nodal point explicitly on a particular  $i$ -level at  $(k + 1)$  th time level. In this way, the values of  $C, T, U$  and  $V$  are obtained at all grid points at time level  $(k + 1)$  th in the region. The process is repeated several times for various  $i$ -level until the steady state is reached. The steady state is assumed to have been reached when the absolute difference between the values of  $U, T$  and  $C$  at two consecutive time steps are less than  $10^{-5}$  at all grid points.

#### 4.0 Results

Numerical computations has been carried out using the method described in the previous section for variations in the fluid parameters, namely Thermal Grashof number  $G_r$ , modified Grashof number  $G_m$ , Magnetic field parameter  $M$ , Heat source parameter  $\gamma$  angle of inclination  $\alpha$ , Prandtl number  $P_r$ , Eckert number  $E_c$  and Schmidt number  $S_c$ . The solutions for the velocity  $U$  versus  $Y$ , Temperature  $\bar{T}$  versus  $Y$ , Concentration  $\bar{C}$  versus  $Y$  are presented in Figs. 2 to 11. Fig. 2 shows the effect of angle of inclination to the vertical direction on the velocity profile for various angles of inclination ( $\alpha = 0^\circ, 30^\circ, 45^\circ, 60^\circ$ ) with fixed values  $P_r = 0.71, S_c = 0.6, M = 0.5, G_r = 20, G_m = 20, \gamma = 0.2$ . From this figure, we observe that the velocity is decreased by increasing the angle of inclination. The fact is that as the angle of inclination increases, the effect of buoyancy force due to thermal diffusion decreases by a factor of  $\cos \alpha$ .

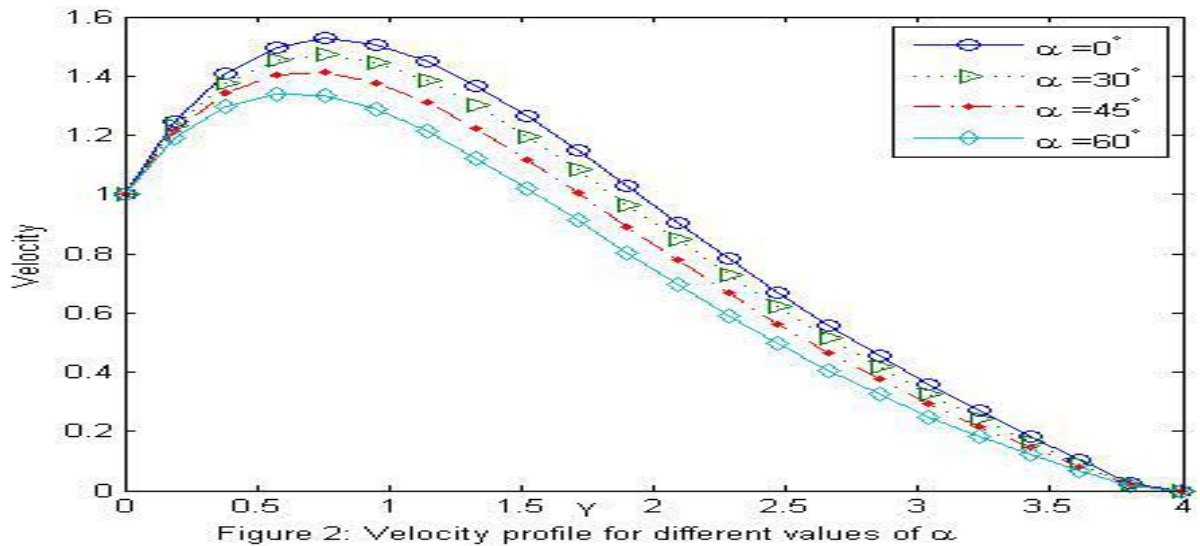


Fig. 3 represents the velocity distributions for different values of Magnetic parameter ( $M = 0.5, 2.5, 4.5$ ) the values of  $P_r = 0.71, S_c = 0.6, G_r = 20, G_m = 20, \gamma = 0.2$ , are constant and with an inclination angle  $0^\circ$ . In this figure, it is observed that velocity distribution decreases with an increase in Magnetic field parameter, since magnetic field exerts a retarding force on fluid flow.

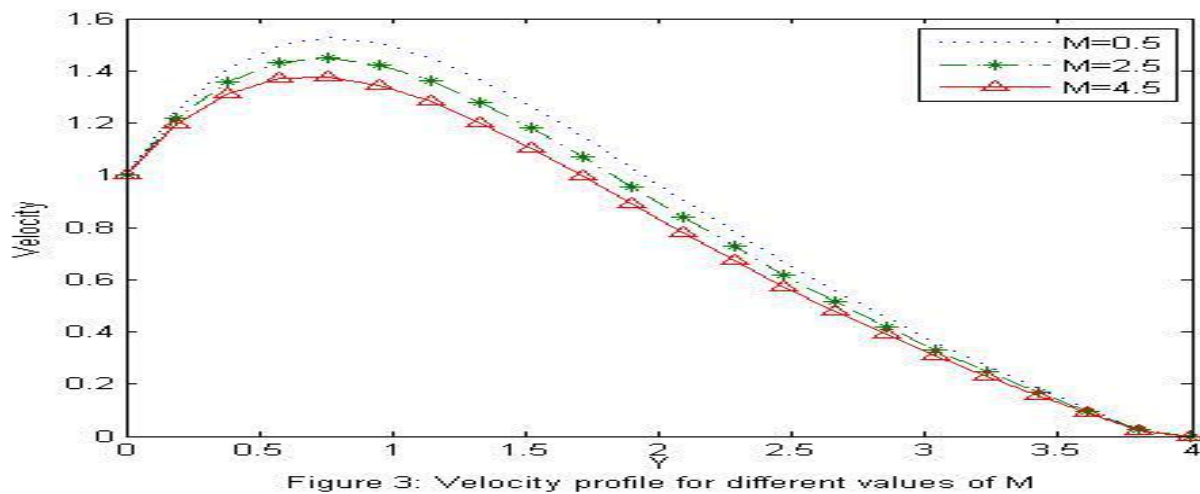


Fig. 4 depicts the velocity distribution for different values of Thermal Grashof number ( $G_r = 20, 30, 40$ ) and the values of  $P_r = 0.71, S_c = 0.6, M = 0.5, G_m = 20, \gamma = 0.2$ , are constants and with an inclination angle  $0^\circ$ . The positive values of  $G_r$  correspond to the cooling of the plate. It is observed that velocity distribution increases with the increase in Grashof numbers.

Fig. 5 shows the velocity distribution for different values of Prandtl number ( $P_r = 0.71, 1.0, 7.0$ ) and the values of  $M = 0.5, G_r = 20, G_m = 20, S_c = 0.6, \gamma = 0.2$  are kept constant with an inclination of  $0^\circ$ . The Prandtl number defines the ratio of momentum diffusivity to thermal diffusivity. The numerical results show that the effect of increasing Prandtl number results in decreasing velocity.

Fig. 6 represents the velocity distribution for different values of Modified Grashof number ( $G_m = 20, 30, 40$ ) and the values of  $G_r = 20, M = 0.5, \gamma = 0.2, S_c = 0.60, P_r = 0.71$  are constant with an inclined angle  $0^\circ$ . The solutant Grashof number  $G_m$  defines the ratio of the species buoyancy force to the viscous hydrodynamic force. The velocity distribution increases with an increase in the solutant Grashof number.



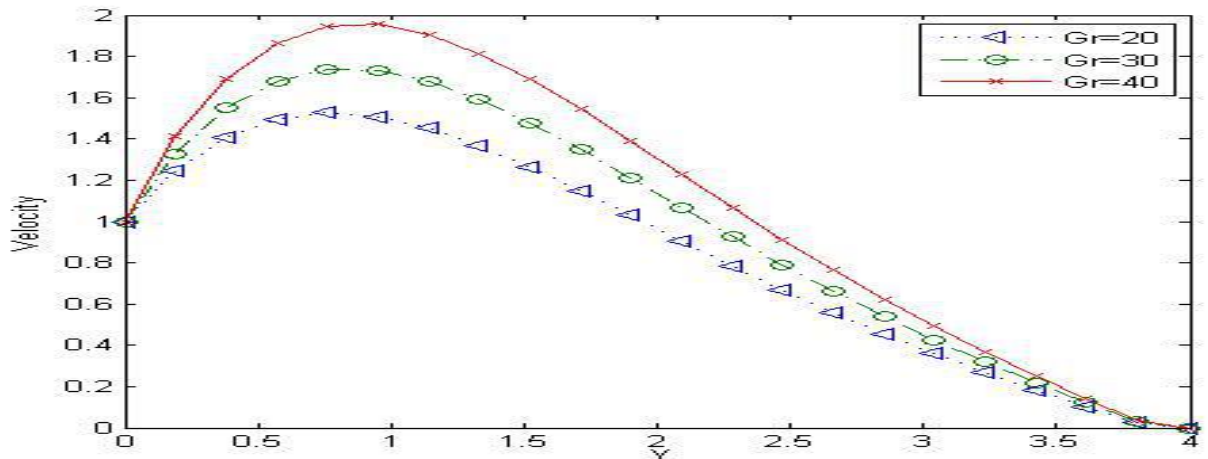


Figure 4 Velocity profile for different values of Gr

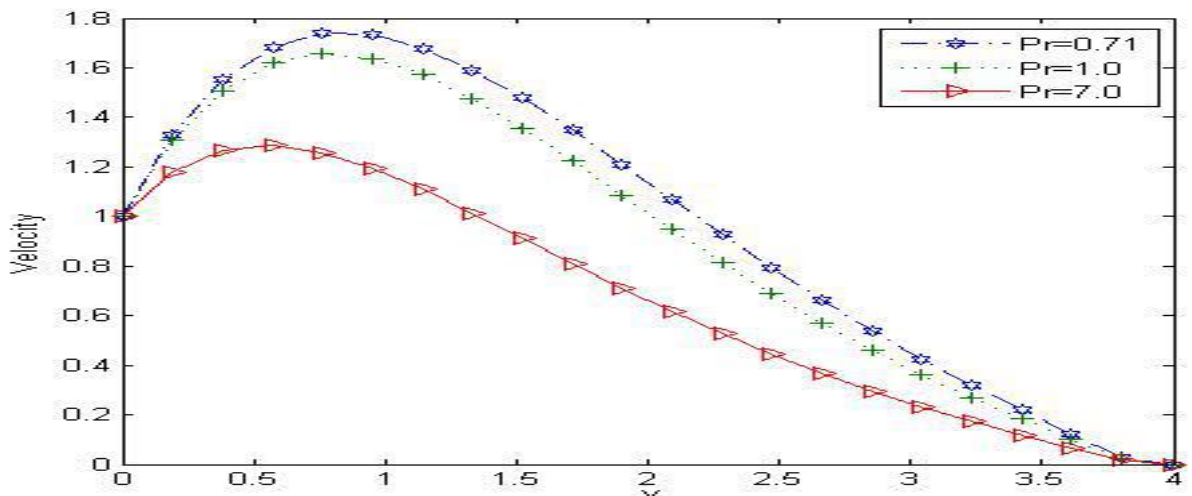


Figure 5: Velocity profile for different values of Pr

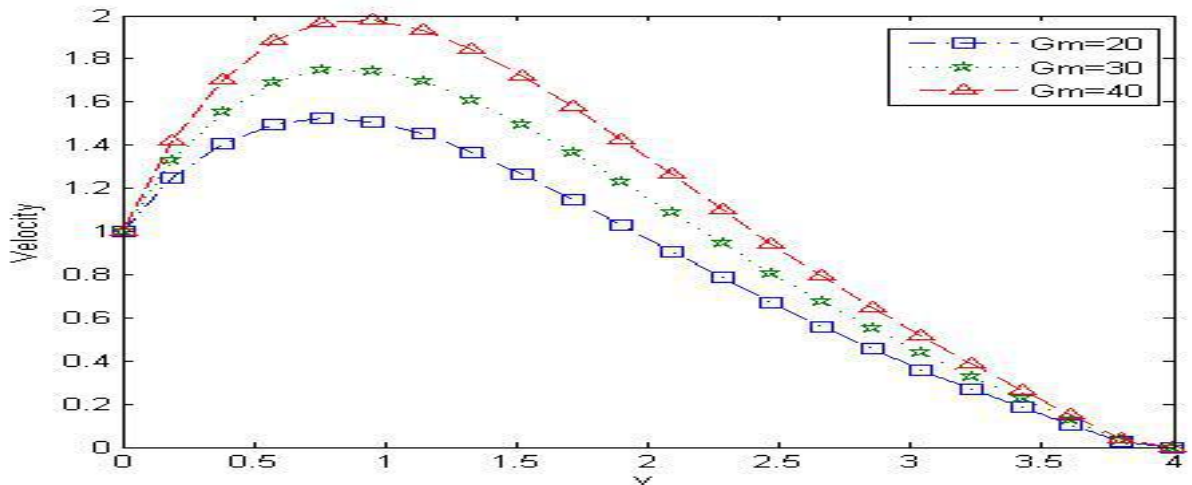


Figure 6: Velocity profile for different values of Gm

Fig. 7 shows the effect of viscous dissipation parameter i.e, the velocity distribution for different values of Eckert number  $E_c = 0.001, 1.0, 1.5, 2.5$  and the values of  $G_r = 20, G_m = 20, M = 0.5, \gamma = 0.2, S_c = 0.60, P_r = 0.71$  are kept unchanged with an inclined angle  $0^\circ$ . The Eckert number  $E_c$  expresses the relationship between the kinetic energy in

the flow and enthalpy. It embodies the conversion of kinetic energy into internal energy by the workdone against the viscous fluid stresses. The positive Eckert number indicates cooling of the plate. i.e loss of heat to the fluid from the plate. It is observed that the velocity distribution increases with the increase in Eckert number. Hence, higher viscous dissipative heat causes a rise in the velocity distribution.

Fig. 8 depicts the temperature distribution for different values of Heat Source parameter ( $\gamma = 0.5, 1.5, 2.5, 3.5$ ) and the values of  $G_r = 20, G_m = 20, M = 0.5, S_c = 0.60, P_r = 0.71$  are constant with an inclined angle  $0^\circ$ . In this figure, it is observed that temperature distribution increases with a rise in Heat source parameter.

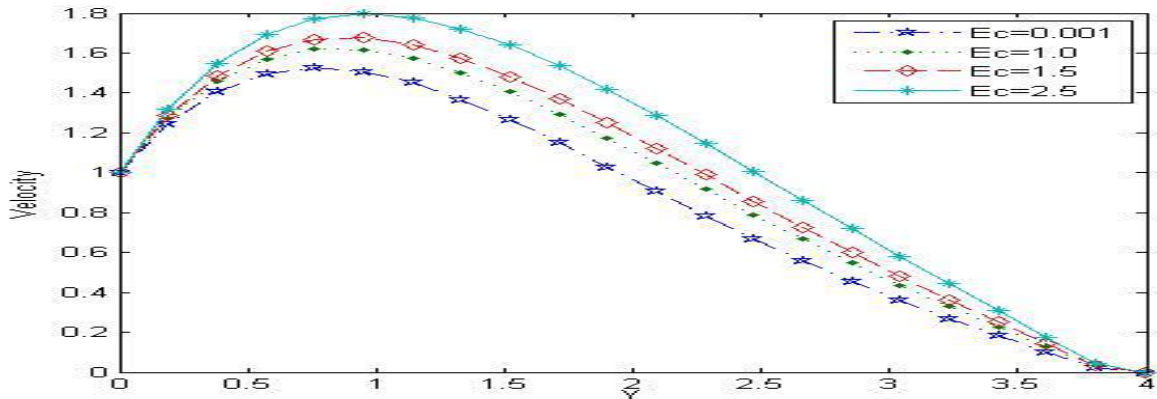


Figure 7: Velocity profile for different values of Ec

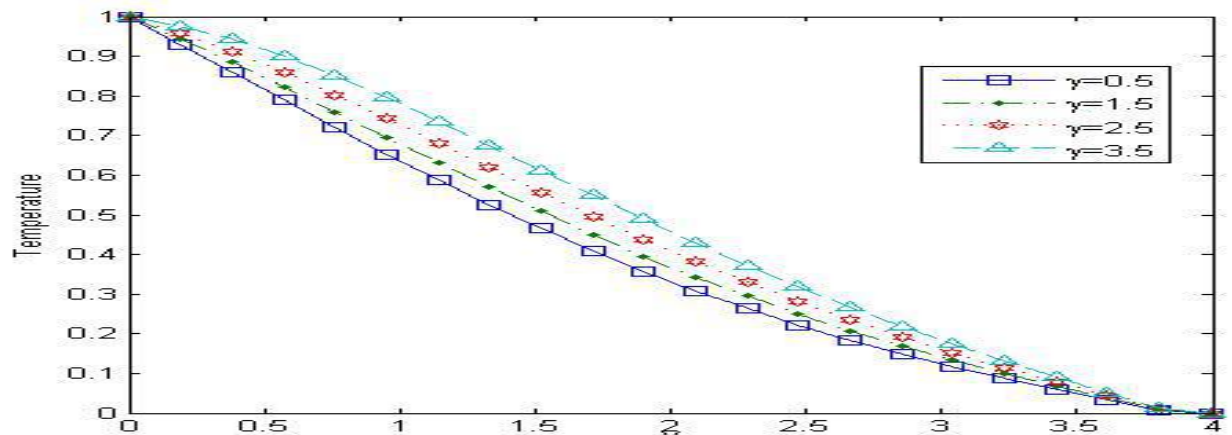


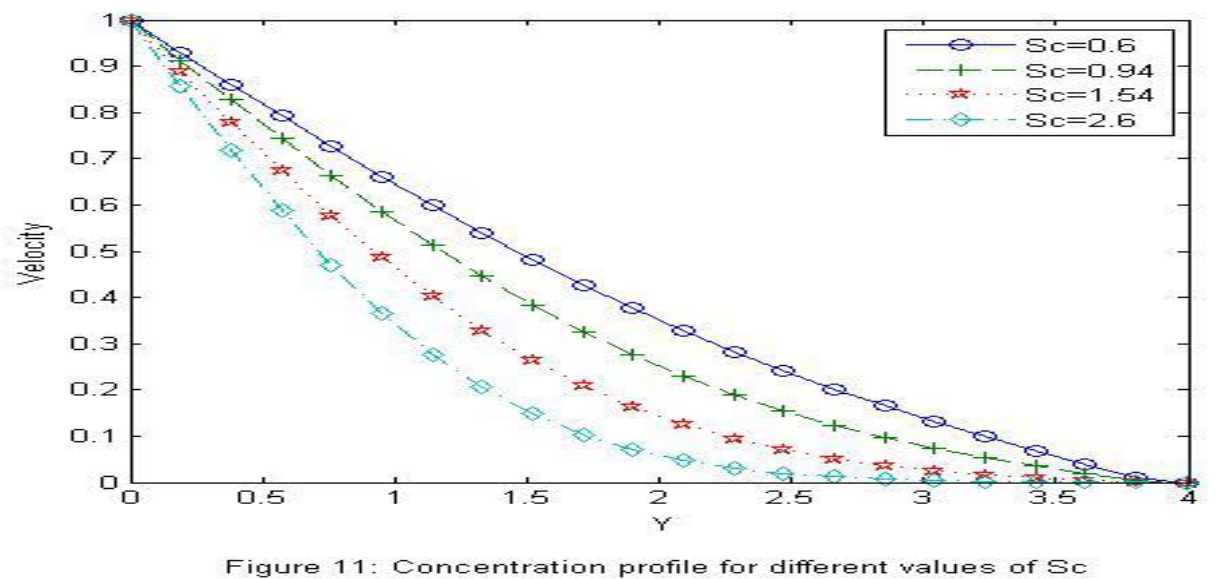
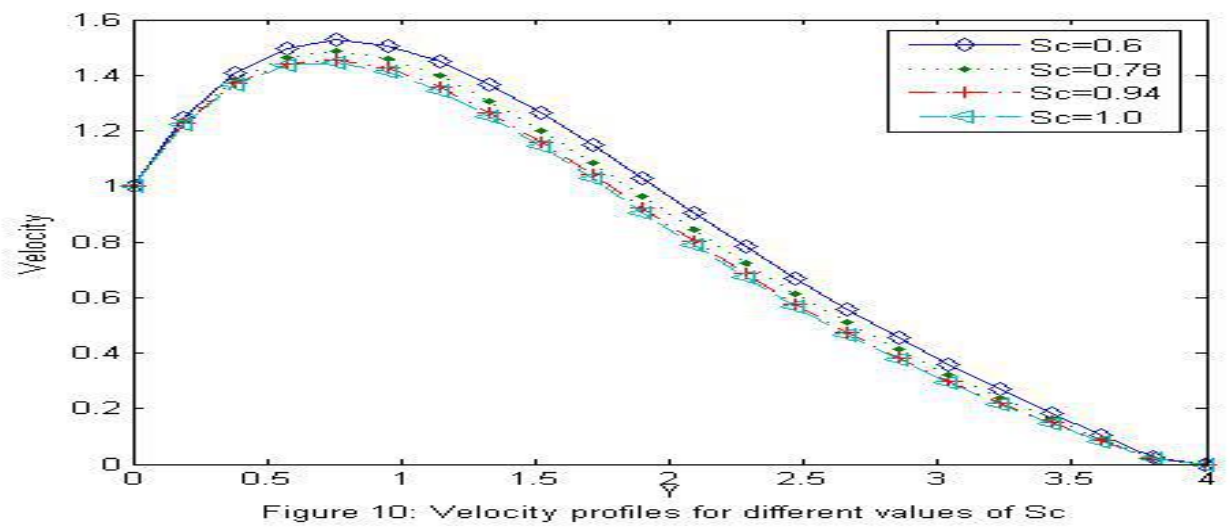
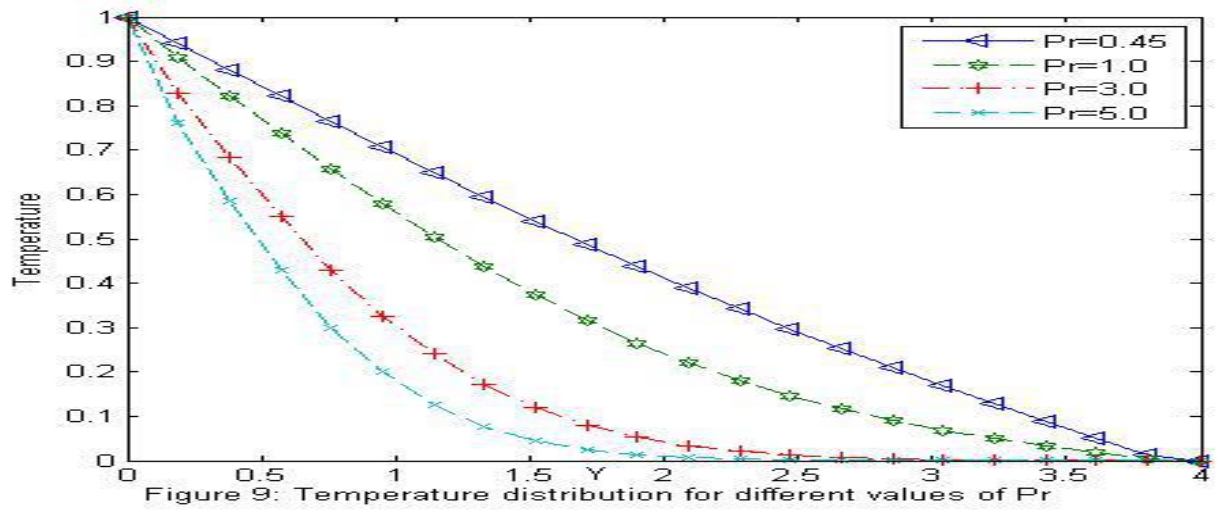
Figure 8: Temperature profile for different values of  $\gamma$

Fig. 9 represents the temperature distribution for different values of Prandtl number ( $P_r = 0.45, 1.0, 3.0, 5.0$ ) and the constant values of  $G_r = 20, G_m = 20, M = 0.5, \gamma = 0.2, S_c = 0.60$  with an inclined angle  $0^\circ$ . The number defines the ratio of momentum diffusivity to thermal diffusivity. It is observed that for smaller values of  $P_r$ , the thermal conductivity increases. It implies that heat is able to diffuse away from the heated plate faster than for higher values of  $P_r$ .

Fig. 10 represents the Velocity profile for different values of Schmidt number. ( $S_c = 0.6, 0.78, 0.94, 1.0$ ) and the constant values of  $G_r = 20, G_m = 20, M = 0.5, \gamma = 0.2, P_r = 0.71$  with an inclined angle  $0^\circ$ . The Schmidt number embodies the ratio of the momentum to the mass diffusivity. It is observed that an increase in the Schmidt number  $S_c$  decreases the velocity.

Fig. 11 represents the Concentration profile for different values of Schmidt number. ( $S_c = 0.6, 0.78, 0.94, 1.0$ ) and the values of  $G_r = 20, G_m = 20, M = 0.5, \gamma = 0.2, P_r = 0.71$  are constant with an inclined angle  $0^\circ$ . It was observed that increase in Schmidt number decreases concentration.





## 5.0 Discussion

The data generated in this study showed the effects of the controlling thermo-physical parameters namely magnetic field ( $M$ ), dissipative function ( $E_c$ ), thermal Grashof number ( $G_r$ ), modified Grashof number ( $G_m$ ), Prandtl number ( $P_r$ ), Schmidt number ( $S_c$ ), Heat source parameter ( $\gamma$ ) and angle of inclination ( $\alpha$ ) on the dimensionless velocity, temperature and concentration profiles are hereby discussed. It was clearly observed that inclination of the plate affects buoyancy force showing that a rise in the inclined angle decreases the buoyancy force. As observed, velocity increased by decreasing magnetic field parameter  $M$ , which implies that the transport rate increases, an indication of the fact that the transverse magnetic field is opposing the transport phenomena. This shows that varying magnetic field parameter results in variation of the Lorentz force which generates more resistance to transport phenomena. This fact agrees very well with findings in earlier reports [4, 7].

The thickness of the thermal boundary layer increased with reduction in  $P_r$ , hence it was noticed that temperature increased with decrease in  $P_r$ . This is due to the fact that smaller values of  $P_r$  are the same as increasing the thermal conductivity of the fluid. Hence, heat diffuses away from the wall faster for higher values of  $P_r$ . In the case of smaller Prandtl numbers, as thermal boundary layer thickens, the heat transfer is reduced.

Two cases of general interest for Grashof number are considered namely  $G_r > 0$  that corresponds to cooling of the plate and  $G_r < 0$  that corresponds to heating of the plate. Evidently, for the positive values of  $G_r$ , the effect of increasing thermal Grashof number or Modified Grashof number manifests an increase in flow velocity. In the presence of Magnetic field parameter, viscous dissipation is demonstrated to have exerted a more significant effect on the flow field and thus affects heat transfer from the plate to the fluid. Velocity and concentration are found to decrease gradually as the Schmidt number increases. The velocity and temperature distribution also increase with an increase in heat source parameter. The viscous dissipative heat parameter ( $E_c$ ) that are often neglected in many investigations and this causes a rise in the velocity of the fluid [4]. This effect on the fluid velocity cannot be played down as shown in this study.

## 6.0 Conclusion

The problem of two-dimensional unsteady magnetohydrodynamics natural convection dissipative flow through an inclined plate has been formulated. The equations governing the model are presented in a non-dimensionalized form and solved using Crank-Nicolson method. Series of computation were carried out in the study and the conclusions drawn are as follows:

- a) The velocity of the fluid decreases as the plate angle increases.
- b) The velocity distribution decreases with an increase in Magnetic field parameter.
- c) Velocity distribution increases with an increase in solutant and thermal Grashof numbers.
- d) A rise in Prandtl number causes a reduction in velocity and temperature distributions.
- e) Higher viscous dissipative heat accelerates the velocity of the fluid.
- f) Temperature distribution increases with a rise in heat source parameter.
- g) An increase in the Schmidt number reduces the velocity of the flow and the concentration of the fluid.

## References

- [1] Mukhopadhyay, S., Layek, G.C. and Samad, S.A. (2005). Study of MHD boundary layer flow over a heated stretching sheet with variable viscosity. *International Journal of Heat Mass Transfer*, Vol.48, pp.4460-4466.
- [2] Gnanaswara R.M. (2012). Lie group analysis of heat and mass transfer effects on steady MHD free convection dissipative fluid flow past an inclined porous surface with heat generation. *Journal of Applied Fluid Mechanics*, Vol. 39, No.3, pp.233-254.
- [3] Gnanaswara, R.M and Bhaskar, R.N. (2011). Mass and Heat generation effects on MHD free convection flow past inclined vertical surface in a porous medium. *Journal of Applied Fluid Mechanics*, Vol. 4, No.3, pp. 7-11.
- [4] Islam, M.S., Samsuzzoha, M.D., Ara, S. and Dey, P. (2013). MHD free convection and mass transfer flow with heat generation through an inclined plate. *Annals of Pure and Applied Mathematics*, Vol. 3, No. 2, pp. 129-141.
- [5] Kalpakides, V.K. and Balassas, K.G. (2004). Symmetry groups and similarity solution for a free convective boundary-layer problem. *International Journal of Non-linear Mechanics*. Vol. 39, No. 10, pp. 1659-1670.
- [6] Sandeep, N. and Sugunamma, V. (2013). Effect of inclined magnetic field on unsteady free convective flow of dissipative fluid past a vertical plate. *World Applied Science Journal*. Vol. 22, No. 7, pp. 975-984.
- [7] Dada, M.S. and Adefolaju, F.H. (2012). Dissipation, MHD and radiation effects on an unsteady convective heat and mass transfer in a Darcy-Forcheimer porous medium. *Journal of Mathematics Research*, Vol. 4, No. 2, pp. 110-127.
- [8] Hunegnaw, D. and Kishan, N. (2014). Unsteady MHD heat and mass transfer flow over stretching sheet in porous medium with variable properties considering viscous dissipation and chemical reaction. *American Chemical Science Journal*, Vol. 4, No.6, pp. 901-917.

- [9] Megahed, A.A., Komy, S.R. and Afify A.A. (2003). Similarity analysis in magnetohydrodynamics hall effects on free convection flow and mass transfer past a semi-infinite vertical flat plate. *International Journal of Non-Linear Mechanics*, Vol. 38, pp. 513-520.
- [10] Ibrahim, F.S., Mansour, M.A. and Hamad, M.A. (2005). Lie group analysis of radiative and magnetic field effects on free convection and mass transfer flow past a semi-infinite vertical flat plate. *Electronic Journal of Differential Equations*, Vol. 39, pp. 1–17.
- [11] Chen, C.H. (2004). Heat and mass transfer in MHD flow by natural convection from a permeable, inclined surface with variable wall temperature and concentration. *Acta Mechanica*, Vol. 172, pp. 219-235.
- [12] Reddy, M.G. and Reddy, N.B. (2011). Mass Transfer and Heat Generation Effects on MHD Free Convection Flow past an Inclined Vertical Surface in a Porous Medium. *Journal of Applied Fluid Mechanics*, Vol. 4, No.1, pp. 7-11.
- [13] Carnahan, B., Luther, H.A. and Willkes, J.O. (1969). *Applied Numerical Method*, John Wiley and Sons, New York, USA.